

Impedance Control Strategy and Experimental Analysis of Collaborative Robots Based on Torque Feedback

Hao Wang

¹*School of Information Science and Technology, University of Science and Technology of China*

²*State Key Laboratory of Robotics, Shenyang Institute of Automation, Chinese Academy of Sciences*

³*Institutes for Robotics and Intelligent Manufacturing, Chinese Academy of Sciences
Hefei, Anhui Province, China
why@mail.ustc.edu.cn*

Zheng Wang and Hongguang Wang

¹*State Key Laboratory of Robotics, Shenyang Institute of Automation, Chinese Academy of Sciences*

²*Institutes for Robotics and Intelligent Manufacturing, Chinese Academy of Sciences*

*Shenyang, Liaoning Province, China
{wzheng & hgwang}@sia.cn*

Abstract - In this paper, through the modeling and analysis of flexible joints, an impedance controller based on torque feedback is proposed, which is used to realize the active compliance of collaborative robots. The controller includes two parts: torque controller and impedance controller. The torque controller is used to compensate the robot dynamics, and the impedance controller is used to adjust the joint stiffness and damping. The theoretical analysis of the control strategy shows that the significance of torque feedback is that it can reshape the inertia of the motor, reduce friction torque and suppress unknown disturbances. In order to ensure tracking accuracy, a task error-based disturbance observer is designed. Experiments with a 7-DOF collaborative robot show that the proposed controller in this paper can realize the body compliance and obtain better compliance performance than the traditional compliance control method.

Index Terms - *Collaborative robots; Torque feedback; Impedance control; Active compliance*

I. INTRODUCTION

A collaborative robot is a kind of robot which can interact directly with human or its environment in a specified cooperative area, which requires the robot body to be flexible enough to ensure the safety of robot interaction with human or its environment. The body compliance of collaborative robots is mainly divided into two categories: passive compliance and active compliance. Passive compliance, defined in paper [1], refers to the method to realize the compliance performance of robot by introducing flexible driver with elastic element. However, this method has problems, such as excessive volume of the flexible joint, complex mechanism and difficulty in realizing a wide range of adjustable rigidity. Therefore, it is difficult to meet the application requirements of the current industrial field. In order to solve the above problems, the effective technology widely used at present is to introduce active compliance control algorithm to realize the compliance performance of robot in the control layer by feedback and response to the contact force information between robot and human or its environment, which has good application value and application prospect.

According to different control ideas, active control is divided into two basic control theories: one is a compliance

control method based on force/position hybrid control proposed in paper [2]. This type of control method introduces a selection matrix to decompose the workspace of the robot into mutually orthogonal force/position control subspaces and control them separately. When the position control is satisfied in some directions, the force interaction is performed in the complementary direction to realize the compliance control of the robot. However, its fundamental disadvantage is that it is unable to perform contact force and position tracking at the same time in the specified direction, and because the method ignores the dynamic coupling between the manipulator and the external environment, the control system instability may be caused.

For the above-mentioned problems, Hogan proposed another control method based on impedance and admittance thought in paper [3]. This control method is proposed from the point of view of energy transmission when the robot is in contact with the environment. By controlling the input flow and the output flow, a dynamic relationship between the external force and the robot motion can be established, which can be represented by the second-order mass (energy storage)-spring (energy storage)-damping (energy consumption) system, and good compliance control effect is obtained. Position-based impedance control, also known as admittance control, is proposed in paper [4]. By introducing an inner loop position controller, the robustness of the controller to factors such as friction that are not accurately modeled is enhanced, but because of the introduction of the inner loop position controller, the following performance of impedance dynamic characteristics decreases. In paper [5] and [6], an impedance control algorithm based on instantaneous model is proposed to overcome the accumulation problem of impedance characteristic following error of admittance control, and the robustness of impedance control to dynamic model and unknown disturbance is improved by introducing inner loop motion controller. However, these classical impedance control methods ignore the flexibility of the robot joint itself, which have a great importance for the design of the tracking controller pointed in paper [7]. Therefore, when these methods are directly applied to collaborative robots with flexible joints, the desired control effect will not be achieved.

In order to solve the above problems, some papers attempt to solve them through advanced control strategies. In paper [8], the robustness analysis and design method of contact task impedance control for flexible manipulator are proposed, and the robust global stability is realized by enhancing the low-order filter in the standard impedance control law. The error compensation is carried out by the reinforcement learning method, and the model-free impedance control in the random position environment is realized in paper [9]. In paper [10], an adaptive impedance control method based on neural network is proposed to approximate the uncertainty of the system, and good simulation results are obtained. However, although the above control methods based on advanced control strategy can sometimes ensure the control effect, the control structure is complex and the stability of the control system is poor, so they are not universal. Therefore, how to design a simple and reliable compliance control method has become one of the challenges in the development of collaborative robots.

In this paper, by modeling and analysis of flexible joints, an impedance control strategy based on torque feedback is proposed, which can realize the active compliance of collaborative robots simply and reliably. This paper is organized as follows. In Section II, the dynamics of flexible joint robot is modeled and analyzed. The design processes of the control strategy based on torque feedback and the task error-based disturbance observer are introduced in Section III. In Section IV, the experiment using a 7-DOF collaborative robot is presented, which proves the effectiveness of the proposed control method and superiority compared to the classical compliance control method. Conclusions are discussed in Section V.

II. DYNAMIC MODELING AND ANALYSIS

The joints of collaborative robots are generally flexible because they contain flexible components such as harmonic reducer and torque sensor. Flexible joints are often expressed in a dual mass model as shown in Fig. 1.

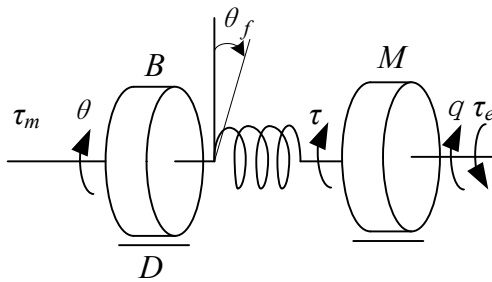


Fig. 1 Dual mass system model.

The elastic element in the flexible joint can be equivalent to the spring in Fig. 1 and K is the equivalent stiffness coefficient. The left side of the spring represents the intrinsic parameter of the motor itself: B represents the inertia of the motor, D is the friction matrix of the motor. The mass block on the right of the spring represents the load of the motor, which inertia is M . The output torque of the motor τ_m causes the motor to rotate the angle θ , the torque τ is transferred to the output side to drive the load rotation through

the elastic element, and the load side rotation angle is q . Assuming that the contact torque between the robot and the environment is τ_e and the friction torque at the motor end is τ_f , the mathematical expression of the flexible joint model is shown as (1).

$$\begin{cases} M(q)\ddot{q} = \tau + \tau_e \\ \tau = K(\theta - q) \\ B\ddot{\theta} + \tau = \tau_m - \tau_f \end{cases} \quad (1)$$

Among them, the motor side friction force τ_f can choose Coulomb-Viscous friction model as shown in (2).

$$\tau_f = \tau_k \text{sgn}(\dot{\theta}) + D_v \dot{\theta} \quad (2)$$

Where, τ_k represents Coulomb friction and D_v represents Viscous friction coefficient.

Consider the robot link inertia and joint flexibility, according to Spong's assumption of flexible joint in [11] and Ott's extension of this hypothesis in [12], the dynamic equation expressed by (1) can be extended to robot dynamics model with flexible joints as shown in (3).

$$\begin{cases} M(q)\ddot{q} + C(q, \dot{q})\dot{q} + g(q) = \tau + DK^{-1}\dot{\tau} + \tau_e \\ \tau = K(\theta - q) \\ B\ddot{\theta} + \tau + DK^{-1}\dot{\tau} = \tau_m - \tau_f \end{cases} \quad (3)$$

The first equation represents the dynamics of the rigid body of the robot, where q is the angular position variable of the link, τ is the output torque of the joint, that is, the driving torque obtained by the link, τ_e is the contact torque between robot and environment, $M(q)$, $C(q, \dot{q})$ and $g(q)$ are inertial term, Coriolis term and gravity term, respectively. The second equation represents the simplified flexibility of joints, where θ is the angular position variable of the motor, and K represents the stiffness coefficient between the flexible joint and the link. The third equation represents the dynamic model of the motor, where τ_m is the output torque of the motor. Comparing (1), it can be seen that the load side of the flexible joint is a strongly coupled and nonlinear rigid-body dynamics model.

III. DESIGN AND ANALYSIS OF CONTROL STRATEGY

In this section, the design process of the control strategy is introduced, and the physical meaning of the torque feedback is given through the analysis of the control strategy. In order to suppress external interference and ensure tracking accuracy, a disturbance observer is designed.

A. Controller design

In order to realize the desired stiffness and damping of robot joints by active compliance control, it is necessary to eliminate the influence of dynamic parameters of robot such as gravity torque, inertia torque, Coriolis torque and friction

torque. Because the load of connecting link is mainly gravity torque at low speed, the controller only identifies the gravity term, while the other terms are compensated by introducing torque feedback. In paper [13], we have proposed a gravity torque identification method based on least square method and QR decomposition, which effectiveness and accuracy have been verified by experiments.

Using the torque signal τ detected by torque sensor as feedback information, the compensation term control law is designed as shown in (4).

$$\tau_{m1} = \tau + K_t(g(q) - \tau) - K_s \dot{\tau} \quad (4)$$

Where, K_t and K_s both are positive definite diagonal matrix coefficients. Substituting (4) into the dynamic model (3) of the flexible robot to obtain the system closed-loop equation as shown in (5).

$$\begin{aligned} \tau_e = & M(q)\ddot{q} + C(q, \dot{q})\dot{q} \\ & + K_t^{-1}B\ddot{\theta} + K_t^{-1}\tau_f \\ & + K_t^{-1}K_s\dot{\tau} + (K_t^{-1} - I)DK^{-1}\dot{\tau} \end{aligned} \quad (5)$$

Where, $M(q)\ddot{q} + C(q, \dot{q})\dot{q}$ is the sum of inertia torque and Coriolis torque on the load side of the motor, which can be ignored when the robot working at low speed. $K_t^{-1}B\ddot{\theta} + K_t^{-1}\tau_f$ is the sum of inertia torque and friction torque on the motor side, and both of them are reduced by K_t times. $K_t^{-1}K_s\dot{\tau} + (K_t^{-1} - I)DK^{-1}\dot{\tau}$ is a differential compensation term, which is used to suppress torque vibration and reduce torque overshoot.

It can be seen from (5) that the gravity term $g(q)$ has been eliminated and the operation of the system is not affected by the gravity term. By adjusting K_t and K_s , the right side of equation (5) can be made very small, which means that the robot can be towed freely with only a small external torque.

In order to make the robot joint exhibit the desired impedance characteristics, the mass-spring-damping model shown in Fig. 2 and its mathematical expression shown in (6) are considered.

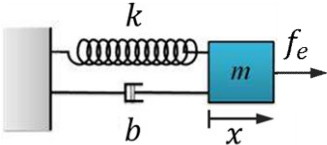
$$f_e = m\ddot{x} + b\dot{x} + kx \quad (6)$$


Fig. 2 Mass-spring-damping model.

The impedance control law of the robot can be obtained by mapping the model to the joint space of the robot and ignoring the inertia term as shown in (7).

$$\tau_{m2} = -K_p \tilde{\theta} - K_d \dot{\tilde{\theta}} \quad (7)$$

Where, K_p and K_d are the expected stiffness coefficient and damping coefficient of the robot joint, and both of them are positive definite diagonal matrices. $\tilde{\theta} = \theta - \theta_d$ represents the error between the actual trajectory and the desired trajectory.

By adding (4) and (7), the impedance control law based on torque feedback can be obtained as shown in (8).

$$\begin{aligned} \tau_m = & \tau_{m1} + \tau_{m2} \\ = & -K_p \tilde{\theta} - K_d \dot{\tilde{\theta}} \\ & + \tau + K_t(g(q) - \tau) - K_s \dot{\tau} \end{aligned} \quad (8)$$

In order to further describe the control system expressed by the control law of (8), the coefficients are transformed as follows.

$$\begin{cases} K_p = BB_\theta^{-1}K_\theta \\ K_d = BB_\theta^{-1}D_\theta \\ K_t = BB_\theta^{-1} - I \\ K_s = (BB_\theta^{-1} - I)DK^{-1} \end{cases} \quad (9)$$

By bringing (9) into (8), we can get another form of (8) as shown in (10).

$$\begin{cases} \tau_m = BB_\theta^{-1}u + (BB_\theta^{-1} - I)(g(q) - 2\tau - DK^{-1}\dot{\tau}) \\ u = -K_\theta \tilde{\theta} - D_\theta \dot{\tilde{\theta}} + \tau \end{cases} \quad (10)$$

where, u is the intermediate control input, B_θ is the positive definite diagonal matrix, and there is $b_{\theta i} < b_i$, the meaning of B_θ will be further explained in the next section. K_θ and D_θ are the positive definite matrices, which represent the stiffness and damping of the impedance controller, respectively. (8) is completely equivalent to (10).

It can be seen from (10) that the control system can be divided into two parts: flexible motor system and rigid body dynamics, where the control law of motor system includes torque compensation controller and impedance controller, which corresponding to (4) and (7), respectively. The control block diagram of the system is shown in Fig. 3.

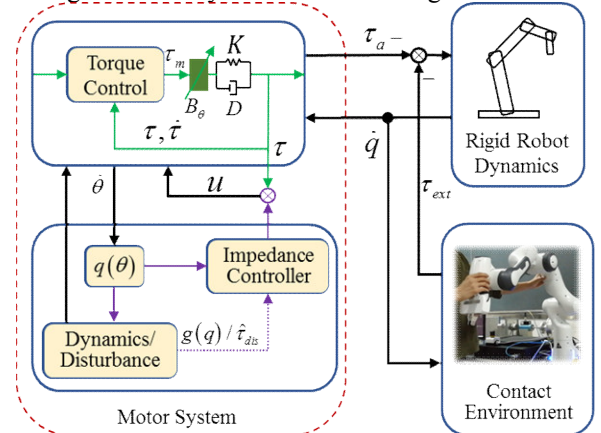


Fig. 3 Impedance control block diagram based on torque feedback.

B. Control strategy analysis

Considering the second equation in the dynamic model (3), (11) can be obtained under quasi-static conditions and ignoring the effect of friction force.

$$\tau = g(q_0) = K(\theta_0 - q_0) \quad (11)$$

Where, θ_0 represent the angle of motor and q_0 represent the angle of connecting rod. It can be seen from (11) that the torque signal τ measured by the torque sensor at low speed is mainly the gravity torque $g(q)$ in the current attitude, that is to say, we can get (12).

$$\tau \approx g(q) \quad (12)$$

(13) can be obtained approximately by bringing (12) into (10).

$$\begin{cases} \tau_m = BB_\theta^{-1}u + (I - BB_\theta^{-1})(\tau + DK^{-1}\dot{\tau}) \\ u = -K_\theta\ddot{\theta} - D_\theta\dot{\theta} + \tau \end{cases} \quad (13)$$

To solve the third formula in the dynamic model (3) and (13), (14) can be obtained.

$$B_\theta\ddot{\theta} + \tau + DK^{-1}\dot{\tau} = u \quad (14)$$

By comparing the third formula in the dynamic model (3) and (14), it can be seen that for the new subsystem with control input u , the effect of torque controller (13) is equivalent to reshaping the inertia of the motor to B_θ . In addition, under the action of torque feedback, any disturbing torque on the motor side is reduced according to the proportion of BB_θ^{-1} , which corresponds to the analysis of torque control in the above.

In paper [14] and [15], the passivity of the system expressed by controller (4) and (13) has been proved. The superposition of passive systems is also passive systems, so the system expressed in (8) is passive, that is, the control system is stable.

C. Task error-based disturbance observer design

In this section, we design a disturbance observer (DOB) based on task error to compensate the nonlinear disturbance caused by the interaction between the robot and the external environment. The principle block diagram of the designed disturbance observer is shown in Fig. 4.

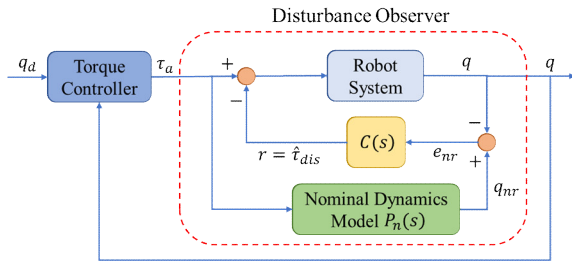


Fig. 4 Principle block diagram of disturbance observer.

Where, e_{nr} is the observation error, $P_n(s)$ is the nominal dynamic model of the robot system. If $C(s)$ defined in PID form as shown in (15).

$$C(s) = -\left(K_1 + K_2s + K_3\frac{1}{s}\right) \quad (15)$$

Then, by (15), the external disturbance estimation $\hat{\tau}_{dis}$ can be obtained as shown in (16).

$$\hat{\tau}_{dis} = -\left(K_1e_{nr} + K_2\dot{e}_{nr} + K_3\int e_{nr}\right) \quad (16)$$

Where, K_1 , K_2 and K_3 are positive definite diagonal matrices.

The performance of the disturbance observer mainly depends on the low-pass filter $Q(s)$. The relationship between $C(s)$ and $Q(s)$ in [16] is as shown in (17).

$$C(s) = \frac{Q(s)}{P_n(s)(Q(s)-1)} \Leftrightarrow Q(s) = \frac{P_n(s)C(s)}{P_n(s)C(s)-1} \quad (17)$$

Using this relation, any $Q(s)$ can be transformed into $C(s)$, and vice versa. The $Q(s)$ filter that corresponds to (17) is a 3-2-order low-pass filter.

III. EXPERIMENT AND ANALYSIS

In this section, a 7-DOF collaborative robot is used to carry out three physical experiments, so as to verify the performance of the designed controller in this paper.

A. Comparison and analysis of compliance performance

In order to analyze the compliance performance of the impedance controller based on torque feedback, a comparative experiment with admittance control is designed. As shown in Fig. 5, we adjust the initial pose of the collaborative robot,

where the joint angle from joint 1 to joint 7 is $0, -\frac{\pi}{4}, 0,$

$-\frac{3\pi}{4}, 0, \frac{\pi}{2}, \frac{\pi}{4}$, and the z axis of Cartesian space is

perpendicular to the ground. The stiffness of the joint 4 is set to 50 Nm/rad and the damping is set to 0. A force F is applied along the z-axis, and then the torque and angle of the joint 4 are read.

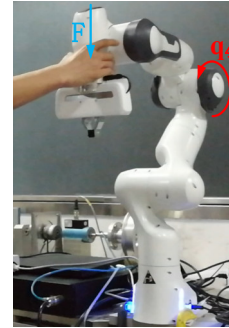


Fig. 5 Stiffness measurement experiment.

During the sampling time of 8s, the collaborative robot is released after applying external force for a period of time to make free oscillation around joint 4. The angle and torque curves of the method proposed in this paper and the admittance control are shown in Fig. 6 and Fig. 7. It can be seen from the curve that after the external force is revoked, the

response of admittance controller quickly decays to the initial position and does not produce the concussion motion, while the response of the controller proposed in this paper produces the concussion motion and gradually decays to the initial position within a period of time. Therefore, impedance control

based on torque feedback is more consistent with the attenuation characteristics of spring concussion motion than admittance control.

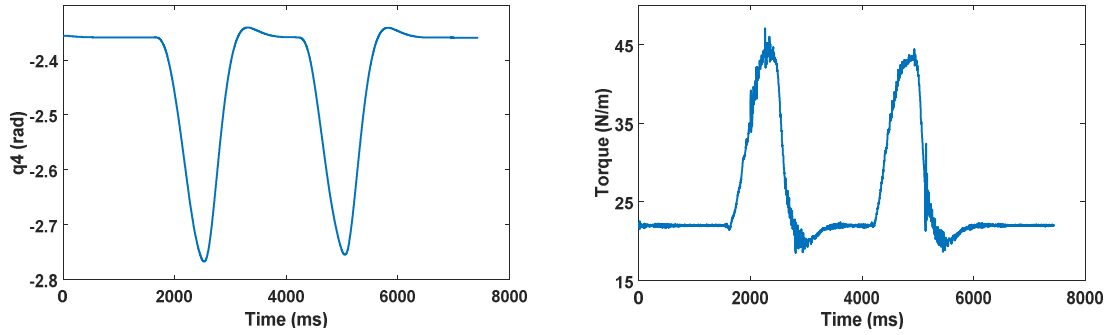


Fig. 6 The angle and torque curve of admittance control.

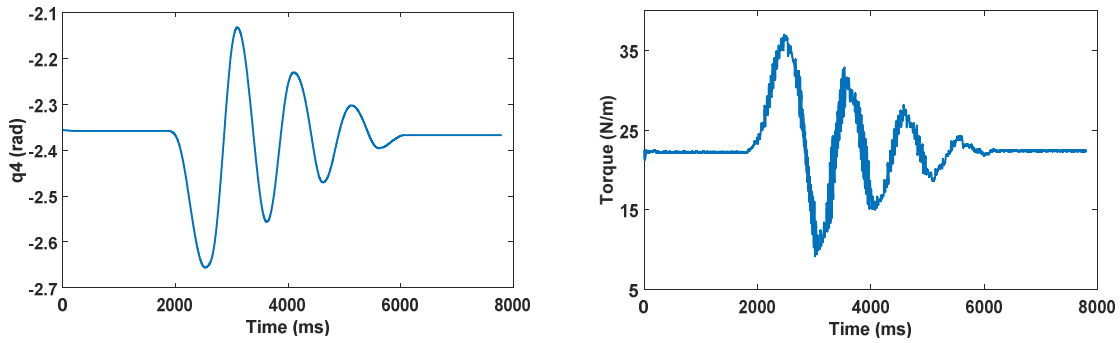


Fig. 7 The angle and torque curve of impedance control based on torque feedback.

In order to intuitively reflect the compliance performance, the change of joint angle and its corresponding joint torque under the action of external force are selected, and the actual joint stiffness is calculated according to the impedance model, as shown in table I and table II. It can be seen from the table data that under the same impedance parameters, the actual joint stiffness of the method proposed in this paper is obviously smaller than that of admittance control, and it is closer to the set joint stiffness parameter, which shows that the compliance performance of impedance control based on torque feedback is obviously better than that of admittance control.

TABLE I
JOINT STIFFNESS OF IMPEDANCE CONTROL
BASED ON TORQUE FEEDBACK

$\Delta q(\text{rad})$	$\Delta \tau(\text{Nm})$	$K(\text{Nm/rad})$
0.2991	14.1112	47.1789
0.2238	11.0014	49.1573
0.2021	9.6182	47.5913

$\Delta q(\text{rad})$	$\Delta \tau(\text{Nm})$	$K(\text{Nm/rad})$
0.3732	21.6534	58.029
0.3466	20.7925	59.9899
0.3526	20.6312	58.5116

B. Robot avoidance based on compliance control

Based on the compliance control theory proposed in this paper, the robot can get the force sensing function, so that

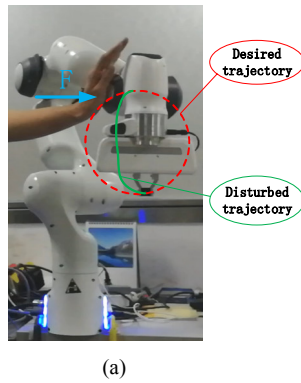
when the robot interacts with human or its environment, the robot can change the desired trajectory of the robot according to the force sensing, and make reasonable avoidance, so as to avoid the robot from being damaged by the collision, or the robot damages the worker. The experimental diagram of the robot based on compliance control is shown in Fig. 8(a), where the red dotted line is the planned desired trajectory and the green curve is the actual trajectory disturbed by external forces.

The angle of joint 1 to 7 of the initial position of the robot is set to $0, -\frac{\pi}{4}, 0, -\frac{3\pi}{4}, 0, \frac{\pi}{2}, \frac{\pi}{4}$. The joint stiffness is set to 100Nm/rad, 100Nm/rad, 50Nm/rad, 25Nm/rad, 25Nm/rad, 10Nm/rad, 5Nm/rad. The joint damping is set to 25Nms/rad, 25Nms/rad, 20Nms/rad, 15Nms/rad, 10Nms/rad, 5Nms/rad, 5Nms/rad. The sampling time is set to 25s. The desired trajectory of Cartesian space is selected as a circle with a radius r in the Y-Z plane. The discrete trajectory is shown in (18).

$$\begin{cases} \theta_i = \theta_{i-1} + T \cdot \frac{v}{r} \\ y_i = y_{i-1} + r \cdot (1 - \cos \theta_i) \\ z_i = z_{i-1} + r \cdot \sin \theta_i \\ r = 0.1 \text{ m} \end{cases} \quad (18)$$

Where, T is the time period of the system, v is the circumferential linear velocity, θ_i is the centrifugal angle of the current time, θ_{i-1} is the centrifugal angle of the upper period, and r is the desired trajectory radius.

The end trajectory of the robot is shown in Fig. 8(b), where the red curve is the desired trajectory, the blue curve is the actual tracking trajectory before the external force disturbance, and the green curve is the actual tracking trajectory after the external force disturbance. It can be seen from the trajectory curve at the end of the robot that when the robot is disturbed by external force, the robot end is obviously deviated from the desired trajectory to avoid excessive contact force with the obstacle. When the external force is revoked,



the actual trajectory at the end of the robot returns to normal under the action of resistance, and continues to track the desired trajectory.

The tracking error curve at the end of the robot is shown in Fig. 9. The red elliptical frame is the tracking error when it is disturbed by external force. It can be seen from the error curve that the robot still has a large tracking error when it is not disturbed by external forces. The main reason is due to the low stiffness of the robot, which leads to the slow response of the system. We have proposed an adaptive control method based on disturbance observer in paper [17], which is used to solve this problem.

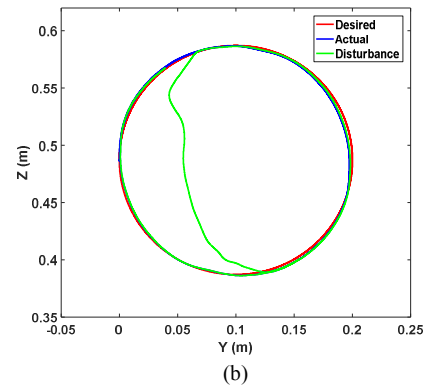


Fig. 8 Robot avoidance based on compliance control.

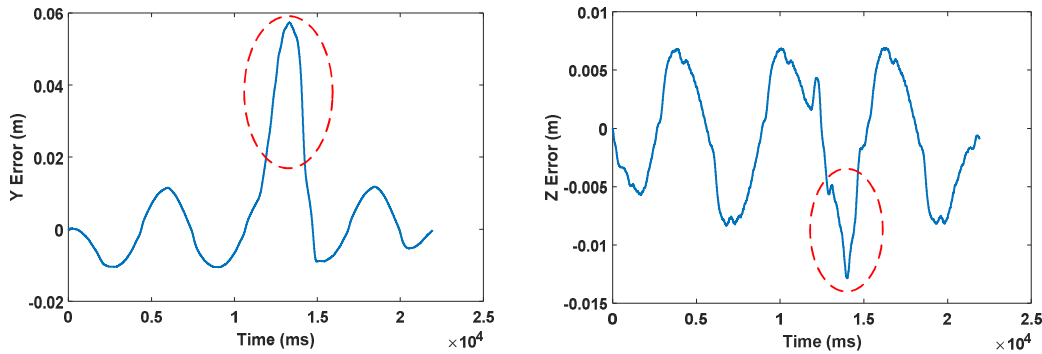


Fig. 9 Tracking error curves of Y and Z axis.

C. Disturbance suppression experiment of observer

In order to verify the suppression effect of the disturbance observer designed in this paper, the step response experiment of the impedance controller proposed in this paper is carried out on a single joint, and the result is shown in Fig. 10, in which the real line and the dotted line represent the results of the controller with observer and the controller without observer, respectively. It can be seen that the steady-state accuracy increases from 0.03° to 0.004° , which means the disturbance observer can effectively suppress the external disturbance of the system.

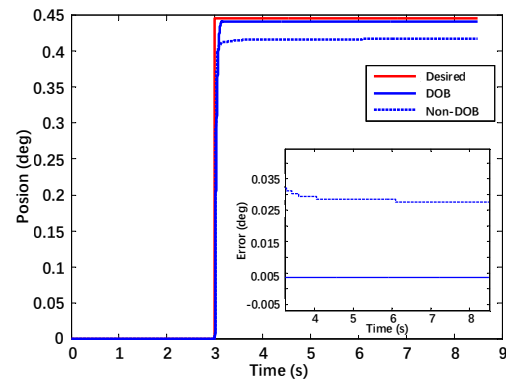


Fig. 10 Comparison curve of step response between controller with DOB and controller without DOB

V. CONCLUSION

In order to solve the compliance control problem of collaborative robots with flexible joints, an impedance control method based on torque feedback is proposed, and the physical meaning of torque controller is given. The control method is robust to robot/load parameters which can't be accurately modeled, so as to maintain good impedance dynamic tracking characteristics and obtain the desired compliance control effect. The effectiveness of the active compliance control method is proved by experiments.

In the next work, we will focus on solving the problem of force tracking in contact space based on the work of this paper, which provides an effective way for collaborative robots to realize the body compliance.

ACKNOWLEDGMENT

This research was supported by Key Projects of Chinese Academy of Sciences (KGZD-EW-608-1) and The State Key Laboratory of Robotics.

REFERENCES

- [1] Wei D. Review of Elastic Actuator Research from Bionic Inspiration[J]. *Jiqiren/Robot*, 2017, 39(4):541-550.
- [2] Mason, Matthew T. Compliance and Force Control for Computer Controlled Manipulators[J]. *IEEE Transactions on Systems, Man and Cybernetics*, 1981, 11(6):418-432.
- [3] Hogan N. Impedance control: An approach to manipulation: Part I—Theory [J]. *Journal of dynamic systems, measurement, and control*, 1985, 107(1): 1-7.
- [4] Pelletier M, Doyon M. On the implementation and performance of impedance control on position controlled robots[C]// *IEEE International Conference on Robotics & Automation*. IEEE, 1994.
- [5] Valency T, Zacksenhouse M. Instantaneous model impedance control for robots[C]// *IEEE/RSJ International Conference on Intelligent Robots & Systems*. 2002.
- [6] Valency T, Zacksenhouse M. Accuracy/robustness dilemma in impedance control[J]. *Journal of dynamic systems, measurement, and control*, 2003, 125(3): 310-319.
- [7] Brogliato B, Ortega R, Lozano R. Global tracking controllers for flexible-joint manipulators: a comparative study[J]. *Automatica*, 1995, 31(7):941-956.
- [8] Wongratanaphisan T, Cole M. Robust Impedance Control of a Flexible Structure Mounted Manipulator Performing Contact Tasks[J]. *IEEE Transactions on Robotics*, 2009, 25(2):445-451.
- [9] Stulp F, Buchli J, Ellmer A, et al. Model-free reinforcement learning of impedance control in stochastic environments[J]. *IEEE Transactions on Autonomous Mental Development*, 2012, 4(4): 330-341.
- [10] He W, Dong Y, Sun C. Adaptive neural impedance control of a robotic manipulator with input saturation[J]. *IEEE Transactions on Systems, Man, and Cybernetics: Systems*, 2016, 46(3): 334-344.
- [11] Spong M W, Khorasani K, Kokotovic P V. An integral manifold approach to the feedback control of flexible joint robots[J]. *IEEE Journal on Robotics & Automation*, 1987, 3(4):291-300.
- [12] Albu-Schaffer A. A Passivity Based Cartesian Impedance Controller for Flexible Joint Robots-part II : Full State Feedback, Impedance Design and Experiments[C]// *Proc. of International Conference on Robotics and Automation, USA 2004-4*. IEEE, 2004.
- [13] Che H, Zheng W, Yiwen Z, et al. Load Adaptive Force-free Control for the Direct Teaching of Robots[J]. *Jiqiren/Robot*, 2017, 39(4):439-448.
- [14] Albu-Schäffer A, Ott C, Hirzinger G. A unified passivity-based control framework for position, torque and impedance control of flexible joint robots[J]. *The international journal of robotics research*, 2007, 26(1): 23-39.
- [15] Ott C, Albu-Schaffer A, Kugi A, et al. On the passivity-based impedance control of flexible joint robots[J]. *IEEE Transactions on Robotics*, 2008, 24(2): 416-429.
- [16] Kim B K, Choi H T, Chung W K, et al. Analysis and design of robust motion controllers in the unified framework[J]. *Transactions-American Society of Mechanical Engineers Journal of Dynamic Systems Measurement and Control*, 2002, 124(2): 313-320.
- [17] Hao Wang, Hongguang Wang, et al. Adaptive Robust Control for Accurate Trajectory Tracking of Collaborative Robots[C]// *IEEE International Conference on CYBER Technology in Automation, Control, and Intelligent Systems*. IEEE, 2019.